tvst

Article

Choroidal Patterns in Retinitis Pigmentosa: Correlation with Visual Acuity and Disease Progression

Alessandro Arrigo[1], Alessandro Bordato[1], Francesco Romano[1,2], Emanuela Aragona[1], Alessio Grazioli[1], Francesco Bandello[1], and Maurizio Battaglia Parodi[1]

[1] Department of Ophthalmology, IRCCS Ospedale San Raffaele, University Vita-Salute, Milan, Italy
[2] Eye Clinic, Department of Biomedical and Clinical Science, Luigi Sacco University Hospital, Milan, Italy

Correspondence: Alessandro Arrigo, Department of Ophthalmology, IRCCS Ospedale San Raffaele, University Vita-Salute, via Olgettina 60, Milan, 20132, Italy. e-mail: alessandro.arrigo@hotmail.com

Received: May 5, 2019
Accepted: December 4, 2019
Published: March 18, 2020

Keywords: retinitis pigmentosa; OCT; OCTA; choroid; Sattler layer; Haller layer

Citation: Arrigo A, Bordato A, Romano F, Aragona E, Grazioli A, Bandello F, Battaglia Parodi M. Choroidal patterns in retinitis pigmentosa: correlation with visual acuity and disease progression. Trans Vis Sci Tech. 2020;9(4):17, https://doi.org/10.1167/tvst.9.4.17

Purpose: The main aim was to identify different choroidal patterns in retinitis pigmentosa (RP) and to assess their clinical and anatomical meanings after 1 year of follow-up.

Methods: Forty-five patients with RP (29 men; mean age 44.5 ± 11.7 years) and 45 healthy controls (29 men; mean age 44.2 ± 9.8 years) were recruited. Optical coherence tomography (OCT) and OCT angiography (OCTA) images were obtained. By means of structural OCT, the following three choroidal patterns were identified: normal-appearing choroid (pattern 1), reduced Haller and Sattler layers (pattern 2), and pattern 2 + choroidal caverns (pattern 3). Main outcome measures were best-corrected visual acuity (BCVA), central macular thickness (CMT), choroidal thickness (CT), vessel density, vessel tortuosity, vessel dispersion, vessel rarefaction, and choroidal stromal index (CSI).

Results: Mean BCVA was 0.27 ± 0.30 LogMAR for patients with RP and 0.0 ± 0.0 LogMAR for controls ($P < 0.01$). CMT, CT, CSI, and OCTA parameters were statistically different between patients with RP and controls ($P < 0.01$). Choroidal patterns 1, 2, and 3 were identified in 20 (44%), 15 (33%), and 10 (23%) patients with RP, respectively. Several statistically significant correlations were also found. Interestingly, after 1 year of follow-up, only the pattern 3 subgroup showed significant worsening of BCVA, CMT, and OCTA parameters ($P < 0.01$).

Conclusions: Choroidal patterns were associated with different RP clinical forms as well as with different progression after 1 year.

Translational Relevance: Choroidal patterns evaluation may provide useful clinical information for patients with RP.

Introduction

Retinitis pigmentosa (RP) includes a group of inherited retinal dystrophies that are characterized by progressive rod-cone degeneration of the photoreceptors, leading to vision deterioration.[1–6]

The pathogenesis of RP is complex, and many factors contribute to the onset and progression of the disease. Generally, loss of photoreceptors and retinal pigmented epithelium (RPE) is followed by impairment at the level of inner retinal neurons, blood vessels, and the optic nerve head.[6–8] Retinal vascular changes, such as arterial narrowing, perivascular cuffing, vessel attenuation, and alterations in vascular blood flow have been described in histopathologic specimens of patients with RP.[9]

Several optical coherence tomography angiography (OCTA) investigations have confirmed the presence of abnormalities in the superficial and the deep retinal capillary plexa (SCP and DCP, respectively), as well as in the choriocapillary (CC) of patients with RP.[10–13] Nevertheless, no study specifically focused on the vascular abnormalities affecting the larger choroidal vessels in RP. The purpose of this study is to analyze the choroidal changes in RP and to correlate the choroidal alterations with the clinical manifestations of RP.

Materials and Methods

The study design is a prospective, observational case series with 1-year follow-up. All the patients were recruited in the Ophthalmology Unit of San Raffaele Hospital (Milan) from October 2016 to December 2017. A signed informed consent was obtained from all patients. The study, conducted in accordance with the Declaration of Helsinki, was approved by the Ethical Committee of the Vita-Salute San Raffaele University in Milan. Consecutive genetically confirmed patients with RP were recruited.

The inclusion criteria were clinical and genetic diagnosis of RP and older than 18 years. The exclusion criteria included high media opacity, any other type of retinal or optic nerve diseases, ophthalmologic surgery within the previous 3 months, refractive error more than ±3D, and any systemic condition potentially affecting the analyses.

Complete ophthalmologic examination included best-corrected visual acuity (BCVA) measurement using standard Early Treatment Diabetic Retinopathy Study (ETDRS) charts, slit-lamp biomicroscopy of anterior and posterior segments, and Goldmann applanation tonometry. Fundus autofluorescence and structural optical coherence tomography (OCT) images were acquired by means of Spectralis HRA+OCT (Heidelberg Engineering, Heidelberg, Germany). Structural OCT acquisition protocol included raster, radial and dense scans with a high number of frames (Automatic Real-time Tracking (ART) ≥30), and enhanced depth imaging (EDI).

An age- and sex-matched control group was considered for clinical and OCT comparisons.

Structural OCT data were used to measure central macular thickness (CMT) and choroidal thickness (CT) at baseline and at 1-year follow-up.

OCTA images were obtained using a swept source OCT DRI Topcon Triton (Topcon Corporation, Tokyo, Japan). OCTA scans included high-resolution 3-mm × 3-mm and 4.5-mm × 4.5-mm acquisitions. Only high-quality images, evaluated by the Topcon Imaging Quality factor >45, were considered.

SCP, DCP, and CC plexa were automatically segmented and carefully inspected by an expert ophthalmologist (MBP), with eventual manual correction. Segmentation boundaries were automatically placed by Topcon software from the upper margin of the retinal nerve fiber layer and the lower margin of the inner plexiform layer for the SCP, from the upper margin of the inner nuclear layer and the lower margin of the outer plexiform layer for the DCP, and from the lower margin of the retinal pigment epithelium and the upper margin of the choroid for the CC. Both macular and optic nerve head reconstructions were considered. In the second case, we included also the automatically segmented layer corresponding to radial peripapillary capillaries, which was included in the retinal nerve fiber layer. All reconstructions were loaded in ImageJ software (National Institutes of Health, Bethesda, MD, USA).[14] In-house scripts were built to calculate the following parameters: vessel density (VD), vessel tortuosity (VT), vessel dispersion (VDisp), and vessel rarefaction (VR), as previously described.[15] Foveal avascular zone was manually segmented and considered within the exclusion criteria. The quantitative evaluation included the measurement of Sattler and Haller layers on a high-resolution, subfoveal, horizontal EDI structural OCT scan and the calculation of the choroidal vascularity index (CVI).[16] Choroidal layers thicknesses were measured by means of five single measures performed beneath the fovea, 750 µm and 1500 µm far from the fovea, on its left and right sides, respectively. The mean measure was considered for the analyses. CVI represented a way to measure the ratio between choroidal vessels and stromal component to quantitatively assess if choroidal vessel impairment occurred in RP. Because we were more focused on the stromal changes occurring in RP, we performed a binarization of structural OCT reconstruction of the choroid; then, we calculated the ratio between black (choroidal vessels) and white pixels (stroma). We named this parameter the choroidal stromal index (CSI). Furthermore, the status of macular external limiting membrane (ELM) and ellipsoid zone was qualitatively assessed at baseline and at follow-up and defined as preserved, disrupted, or absent.[17] This analysis was made on the same structural OCT horizontal scan centered on the fovea.

Two expert blinded graders (FR, AA) classified three different choroidal patterns on the basis of choroidal layer thicknesses and CSI. In particular, pattern 1 was similar to the pattern in healthy participants, pattern 2 was characterized by reduced Sattler and Haller layers and reduced CSI, and pattern 3 showed reduced Sattler and Haller layers with choroidal caverns and reduced CSI. The agreement of the two graders was 95%. Uncertain cases were analyzed by a third author (AG).

The statistical analyses were performed using the one-way analysis of variance test with Bonferroni correction for multiple comparisons (SPSS, Chicago, IL, USA), with statistical significance set at $P < 0.05$.

Tau–Kendall correlation analysis (SPSS) was used to assess the statistical relationships between the following parameters: BCVA, CMT, CT, VD, VT, VR, and VDisp.

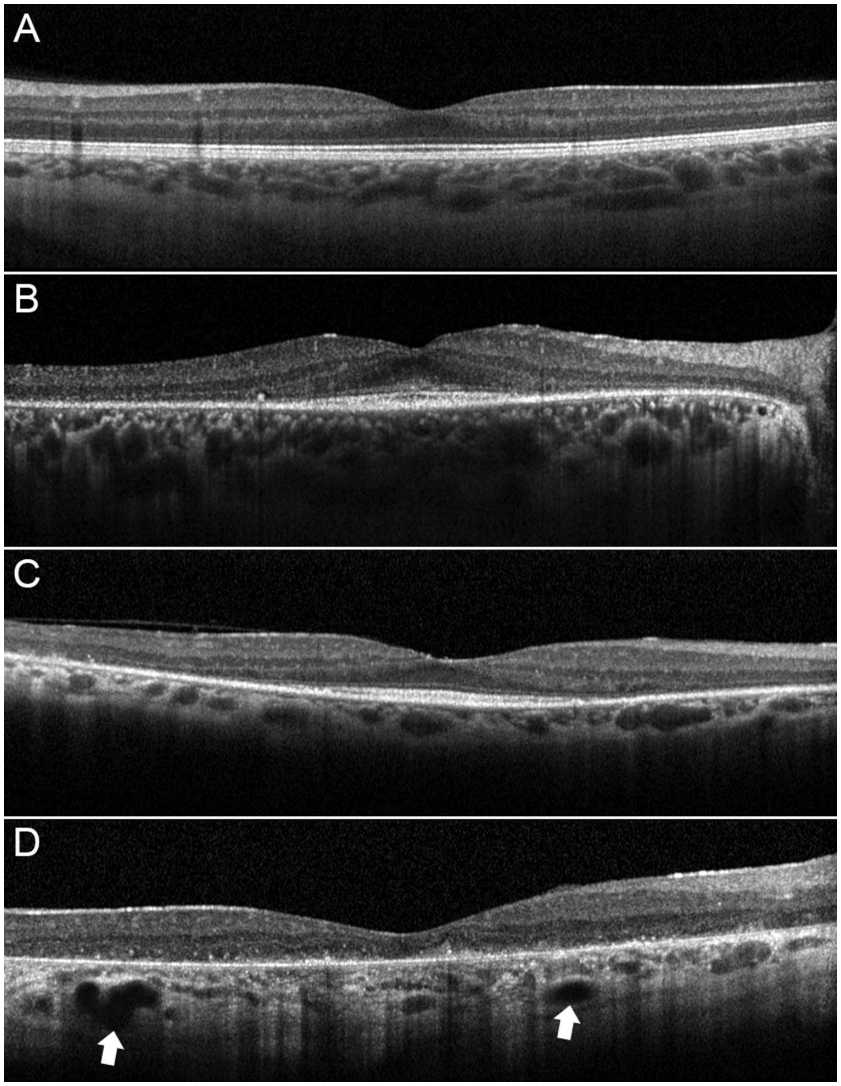

Figure 1. Choroidal patterns in RP. If compared with a control participant (A), pattern 1 is characterized by normal-appearing choroidal vessels (B). Pattern 2 disclosed reduced Haller and Sattler layers (C). Pattern 3 showed also the presence of choroidal caverns (*white arrows*) (D). It is worth noticing the increase of choroidal hyperreflective signal, interpretable as an enlargement of a stromal component.

Results

Overall, 50 consecutive patients with a clinically and genetically confirmed diagnosis of RP were enrolled. Three patients were excluded for high media opacities and two patients because of systemic conditions potentially affecting the results of the study (one with uncontrolled arterial hypertension and another with diabetes mellitus).

Forty-five eyes (45 patients) were included in our analysis (29 men; mean age 44.5 ± 11.7 years). Moreover, 45 healthy control participants (29 men; mean age 44.2 ± 9.8 years) were also included. Mean BCVA was 0.27 ± 0.30 LogMAR for the RP group and 0.0 ± 0.0 LogMAR for controls ($P < 0.01$). Based on structural OCT classification (Fig. 1), patterns 1, 2, and 3 were identified in 20 (44%), 15 (33%), and 10 (23%) patients with RP, respectively. Complete data are listed in Table 1. Pattern 1 turned out to be characterized by better clinical and OCTA outcomes. Eyes showing pattern 1 had higher BCVA, VD, and VT and lower VDisp and VR, if considering both macular and optic nerve head parameters, if compared with pattern 2 and pattern 3. All pattern 1 parameters were statistically worse than those of controls ($P < 0.05$), except for VD of macular CC, nerve SCP, and nerve CC ($P > 0.05$). On the other side, pattern 2 showed in most of the cases not significantly different parameters with respect to pattern 3, including BCVA.

Table 1. RP Subgroups Analysis

Parameter	Choroidal Pattern	Mean	SD	*P* Values					
Age	1	38	12	1 vs. 2	1 vs. 3	2 vs. 3		All RP vs. controls	
	2	45	8						
	3	48	7	0.121	0.135	0.428		0.553	
	Controls	44	10						
RNFL	1	99	12	1 vs. 2	1 vs. 3	2 vs. 3	1 vs. controls	2 vs. controls	3 vs. controls
	2	73	15						
	3	65	11	**<0.01**	**<0.01**	0.634	**<0.05**	**<0.01**	**<0.01**
	Controls	101	9						
CMT	1	244	22	1 vs. 2	1 vs. 3	2 vs. 3		All RP vs. controls	
	2	204	26						
	3	201	21	**<0.01**	**<0.01**	0.445		**<0.01**	
	Controls	302	19						
Choroidal thickness	1	227	37	1 vs. 2	1 vs. 3	2 vs. 3		All RP vs. controls	
	2	218	43						
	3	156	40	**<0.01**	**<0.01**	**<0.01**		**<0.01**	
	Controls	305	59						
BCVA (LogMAR)	1	0.04	0.09	1 vs. 2	1 vs. 3	2 vs. 3	1 vs. controls	2 vs. controls	3 vs. controls
	2	0.42	0.27						
	3	0.57	0.26	**<0.01**	**<0.01**	>0.05	**<0.05**	**<0.01**	**<0.01**
	Controls	0.0	0.0						
VD mSCP	1	0.40	0.02	1 vs. 2	1 vs. 3	2 vs. 3	1 vs. controls	2 vs. controls	3 vs. controls
	2	0.39	0.01						
	3	0.38	0.02	<0.01	<0.01	0.323	**<0.05**	**<0.01**	**<0.01**
	Controls	0.41	0.01						

Table 1. Continued

Parameter	Choroidal Pattern	Mean	SD	*P* Values					
VD mDCP	1	0.38	0.02	1 vs. 2	1 vs. 3	2 vs. 3		All RP vs. controls	
	2	0.36	0.02						
	3	0.33	0.03	0.225	**<0.01**	**<0.01**		**<0.01**	
	Controls	0.43	0.01						
VD mCC	1	0.50	0.02	1 vs. 2	1 vs. 3	2 vs. 3	1 vs. controls	2 vs. controls	3 vs. controls
	2	0.48	0.01						
	3	0.47	0.01	**<0.01**	**<0.01**	0.365	0.855	**<0.01**	**<0.01**
	Controls	0.50	0.01						
VD RPC	1	0.44	0.02	1 vs. 2	1 vs. 3	2 vs. 3	1 vs. controls	2 vs. controls	3 vs. controls
	2	0.40	0.03						
	3	0.40	0.03	**<0.01**	**<0.01**	0.865	**<0.05**	**<0.01**	**<0.01**
	Controls	0.45	0.01						
VD nSCP	1	0.43	0.01	1 vs. 2	1 vs. 3	2 vs. 3	1 vs. controls	2 vs. controls	3 vs. controls
	2	0.40	0.02						
	3	0.41	0.01	**<0.01**	**<0.01**	0.125	0.425	**<0.01**	**<0.01**
	Controls	0.43	0.01						
VD nDCP	1	0.30	0.01	1 vs. 2	1 vs. 3	2 vs. 3		All RP vs. controls	
	2	0.31	0.04						
	3	0.29	0.01	0.445	0.321	0.145		**<0.01**	
	Controls	0.40	0.02						
VD nCC	1	0.54	0.02	1 vs. 2	1 vs. 3	2 vs. 3	1 vs. controls	2 vs. controls	3 vs. controls
	2	0.50	0.05						
	3	0.46	0.02	**<0.01**	**<0.01**	**<0.01**	>0.473	**<0.01**	**<0.01**
	Controls	0.54	0.03						

Table 1. Continued

Parameter	Choroidal Pattern	Mean	SD	*P* Values			
Vdisp mSCP	1	11.92	2.45	1 vs. 2	1 vs. 3	2 vs. 3	All RP vs. controls
	2	18.17	12.48				
	3	21.91	15.16	0.251	**<0.01**	0.114	**<0.01**
	Controls	10.72	4.15				
Vdisp mDCP	1	14.76	7.99	1 vs. 2	1 vs. 3	2 vs. 3	All RP vs. controls
	2	34.37	9.96				
	3	26.61	10.47	**<0.01**	**<0.01**	0.521	**<0.01**
	Controls	11.45	3.48				
Vdisp RPC	1	23.86	5.22	1 vs. 2	1 vs. 3	2 vs. 3	All RP vs. controls
	2	37.85	16.15				
	3	40.76	16.69	**<0.01**	**<0.01**	>0.234	**<0.01**
	Controls	10.61	3.70				
Vdisp nSCP	1	23.34	10.53	1 vs. 2	1 vs. 3	2 vs. 3	All RP vs. controls
	2	34.90	12.19				
	3	26.89	13.50	0.190	0.251	0.145	**<0.01**
	Controls	10.35	2.88				
Vdisp nDCP	1	25.20	8.38	1 vs. 2	1 vs. 3	2 vs. 3	All RP vs. controls
	2	36.15	11.35				
	3	42.35	13.89	**<0.01**	**<0.01**	0.205	**<0.01**
	Controls	10.37	3.36				
VT mSCP	1	5.17	0.31	1 vs. 2	1 vs. 3	2 vs. 3	All RP vs. controls
	2	4.64	0.26				
	3	4.54	0.10	**<0.01**	**<0.01**	0.198	**<0.01**
	Controls	7.20	0.31				

Table 1. Continued

Parameter	Choroidal Pattern	Mean	SD	*P* Values			
VT mDCP	1	5.08	0.41	1 vs. 2	1 vs. 3	2 vs. 3	All RP vs. controls
	2	4.26	0.28				
	3	4.09	0.34	**<0.01**	**<0.01**	0.333	**<0.01**
	Controls	7.84	0.34				
VT RPC	1	5.47	0.40	1 vs. 2	1 vs. 3	2 vs. 3	All RP vs. controls
	2	4.71	0.19				
	3	4.90	0.29	**<0.01**	**<0.01**	0.249	**<0.01**
	Controls	7.73	0.30				
VT nSCP	1	5.51	0.35	1 vs. 2	1 vs. 3	2 vs. 3	All RP vs. controls
	2	4.74	0.46				
	3	4.93	0.19	**<0.01**	**<0.01**	0.341	**<0.01**
	Controls	8.42	0.33				
VT nDCP	1	4.34	0.46	1 vs. 2	1 vs. 3	2 vs. 3	All RP vs. controls
	2	4.05	0.42				
	3	3.90	0.41	0.661	0.459	0.354	**<0.01**
	Controls	7.06	0.25				
VR mSCP	1	0.63	0.04	1 vs. 2	1 vs. 3	2 vs. 3	All RP vs. controls
	2	0.69	0.03				
	3	0.69	0.02	**<0.01**	**<0.01**	0.849	**<0.01**
	Controls	0.41	0.01				
VR mDCP	1	0.60	0.03	1 vs. 2	1 vs. 3	2 vs. 3	All RP vs. controls
	2	0.64	0.03				
	3	0.64	0.04	**<0.01**	**<0.01**	0.851	**<0.01**
	Controls	0.43	0.01				

Table 1. Continued

Parameter	Choroidal Pattern	Mean	SD	*P* Values			
VR RPC	1	0.60	0.08	1 vs. 2	1 vs. 3	2 vs. 3	All RP vs. controls
	2	0.65	0.04				
	3	0.69	0.02	0.05	**<0.01**	0.444	**<0.01**
	Controls	0.47	0.01				
VR nSCP	1	0.62	0.05	1 vs. 2	1 vs. 3	2 vs. 3	All RP vs. controls
	2	0.67	0.04				
	3	0.71	0.03	0.164	**<0.01**	0.223	**<0.01**
	Controls	0.46	0.01				
VR nDCP	1	0.48	0.06	1 vs. 2	1 vs. 3	2 vs. 3	All RP vs. controls
	2	0.55	0.07				
	3	0.53	0.03	0.105	0.114	0.641	**<0.01**
	Controls	0.42	0.01				

"m" and "n" used for macular and optic nerve head vascular plexa, respectively. RNFL, retinal nerve fibers layer; RPC, radial peripapillary capillaries. Bold values highlight statistically significant values.

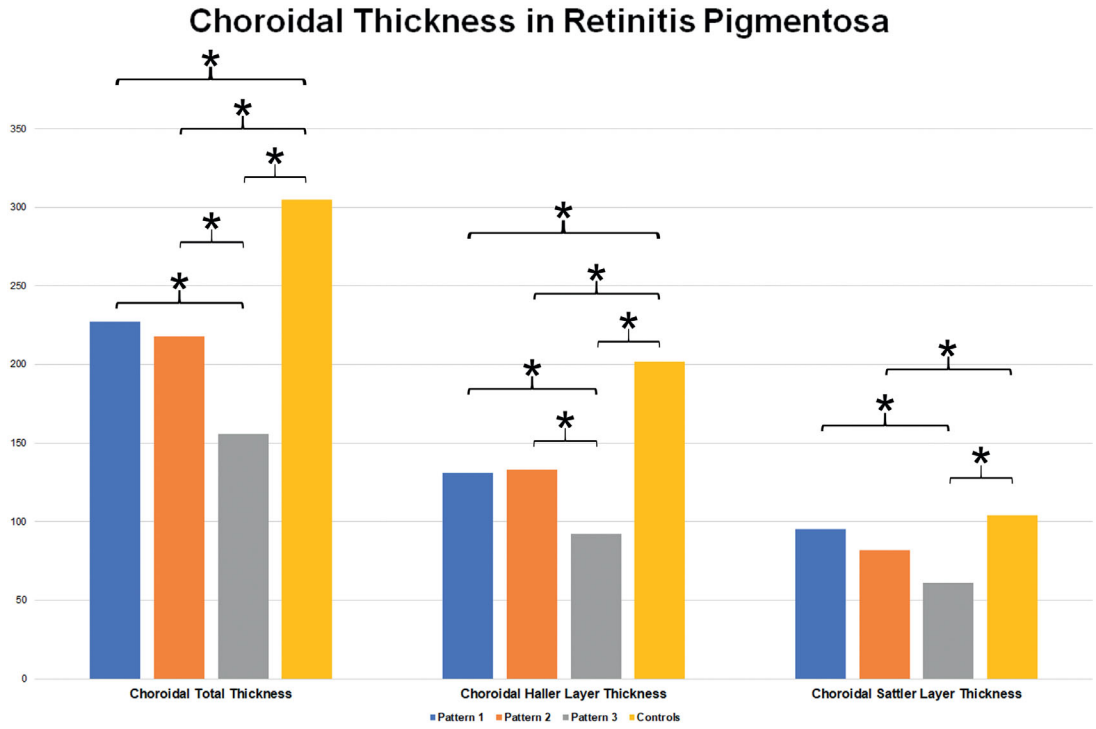

Figure 2. Choroidal thickness analysis in RP. Statistically significant differences are marked by *asterisks*.

Interestingly, the choroid was statistically thicker in pattern 2 than in pattern 3. Tau–Kendall correlation analysis confirmed the relationship between choroidal patterns and the worsening of quantitative parameters (Table 2). Indeed, lower choroidal patterns were associated with better BCVA, higher VD and VT parameters, and lower VR and VDisp parameters.

Interestingly, CSI analysis showed no statistically significant differences between control subjects and pattern 1 ($P > 0.05$). On the contrary, pattern 2 and pattern 3 showed a significant increase of CSI, if compared both with controls and pattern 1 ($P < 0.01$). Choroidal total thickness was significantly different among all the subgroups ($P < 0.01$), with the only exception of pattern 1 versus pattern 2 ($P > 0.05$). In detail, Haller layer was statistically altered in all RP patterns ($P < 0.01$), whereas Sattler layer appeared not significantly involved in pattern 1, with respect to control subjects ($P > 0.05$). Both Haller and Sattler choroidal layers were not statistically different between pattern 1 and pattern 2 ($P > 0.05$). All data are extensively reported in Table 3 and Figure 2.

After 1 year of follow-up, average BCVA slightly worsened to 0.33 ± 0.39 LogMAR ($P = 0.45$), whereas the same choroidal patterns were maintained in all eyes. However, only the pattern 3 subgroup showed significant worsening of VD and VT parameters, both for macular and optic nerve head plexa (Table 4). In detail, BCVA decreased from 0.57 ± 0.26 LogMAR to 0.83 ± 0.29 LogMAR, and CMT decreased from 201 $\pm$ 21 µm to 179 $\pm$ 21 µm, along with the deterioration of almost all the VD and VT values. In addition, the condition of ELM and ellipsoid zone turned out to worsen only in the pattern 3 subgroup, with a documented deterioration in 70% of cases, against the 40% detected at baseline (Fig. 3). This deterioration was documented by increased reflectivity attenuation of the outer retinal layers, together with an increased window effect secondary to the atrophy of the RPE.

Discussion

Choroidal blood vessels can be divided into the Sattler layer, which is in continuity with the choriocapillaris, and the Haller layer, located on the scleral side. Previous studies already reported choroidal thinning in RP with respect to healthy controls.[18,19] However, at present, no study has thoroughly investigated the choroidal features in RP with their clinical correlations.

In the present study, based on the structural OCT findings, we identified three choroidal patterns: normal-appearing choroid (pattern 1), reduced Haller and Sattler layers (pattern 2), and reduced Haller and Sattler layers with choroidal caverns (pattern 3).

Table 2. Correlation Analysis of Choroidal Patterns in RP

		RNFL	CMT	BCVA (logMAR)	VD mSCP	VD mDCP	VD mCC	VD RPC	VD nSCP	VD nCC	Vdisp mDCP	Vdisp RPC	Vdisp nDCP	VT mSCP	VT mDCP	VT RPC	VT nSCP	VT nDCP	VR mSCP	VR mDCP	VR RPC	VR nSCP	VR nDCP
Choroidal pattern	Tau coefficient	−0.641	−0.513	0.757	−0.439	−0.557	−0.576	−0.432	−0.469	−0.631	0.442	0.355	0.455	−0.599	−0.647	−0.484	−0.519	−0.333	0.5	0.423	0.503	0.519	0.295
	P value	**<0.01**	**<0.01**	**<0.01**	**<0.01**	**<0.01**	**<0.01**	**<0.01**	**<0.01**	**<0.01**	**<0.01**	**<0.01**	**<0.01**	**<0.01**	**<0.01**	**<0.01**	**<0.01**	**<0.01**	**<0.01**	**<0.01**	**<0.01**	**<0.01**	**<0.01**

"m" and "n" used for macular and optic nerve head vascular plexa, respectively.

Table 3. Quantitative Analysis of Choroidal Imaging Features in RP

					P Value					
	Pattern 1	Pattern 2	Pattern 3	Controls	Control vs. P1	Control vs. P2	Control vs. P3	P1 vs. P2	P1 vs. P3	P2 vs. P3
Choroidal stromal index										
Mean	0.03	0.07	0.09	0.03	0.685	**<0.01**	**<0.01**	**<0.01**	**<0.01**	0.354
SD	0.01	0.01	0.05	0.01						
Choroidal total thickness										
Mean	227	218	156	305	**<0.01**	**<0.01**	**<0.01**	0.416	**<0.01**	**<0.01**
SD	37	44	40	59						
Choroidal Haller layer thickness										
Mean	131	133	92	202	**<0.01**	**<0.01**	**<0.01**	0.555	**<0.01**	**<0.01**
SD	26	26	28	48						
Choroidal Sattler layer thickness										
Mean	95	82	61	104	0.217	**<0.01**	**<0.01**	0.134	**<0.01**	0.368
SD	22	24	31	27						

Bold values highlight statistically significant values.

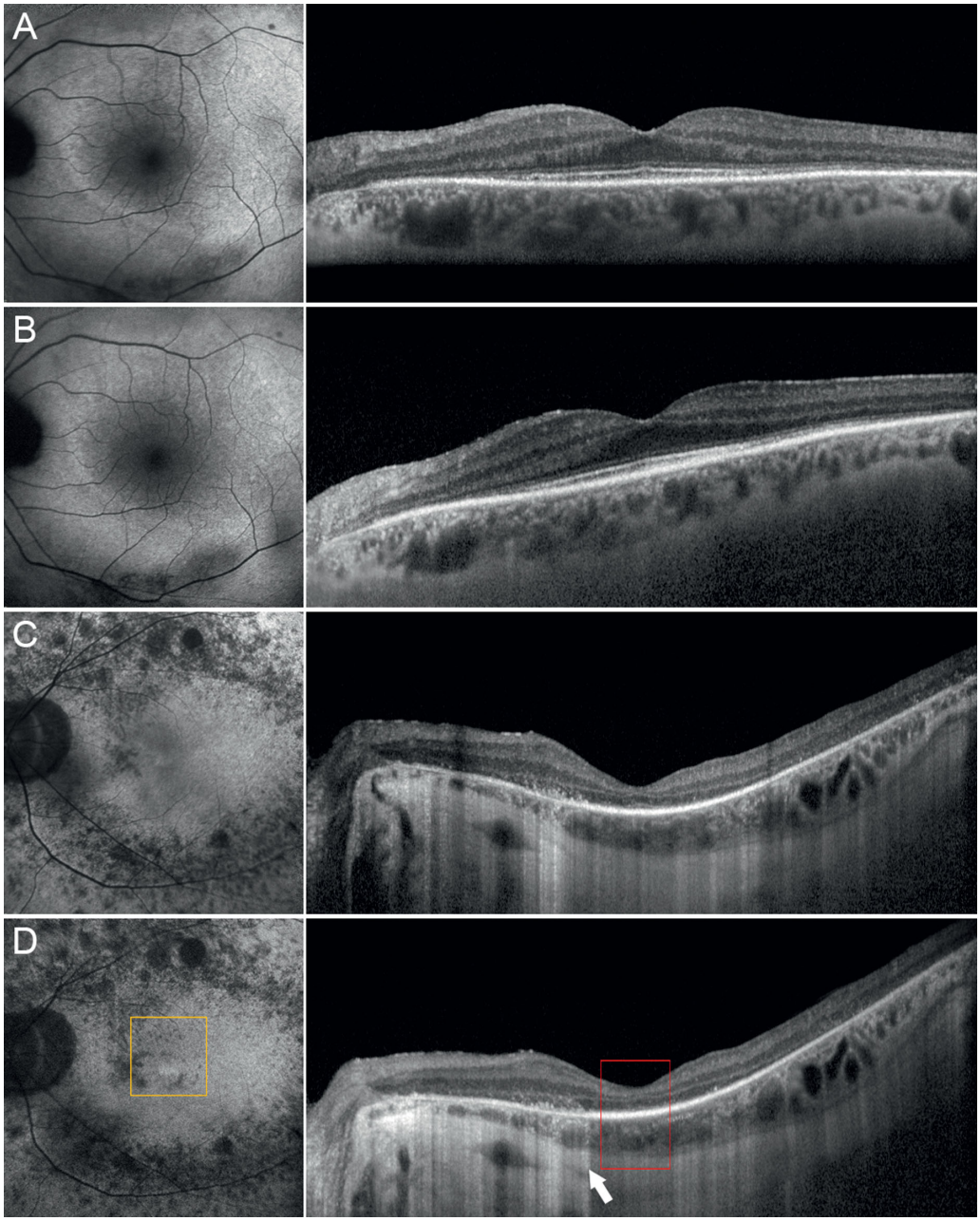

Figure 3. One-year follow-up and RP progression. Pattern 1 showed unremarkable changes if looking at baseline features (A) and 1-year follow-up (B). On the contrary, pattern 3 showed a remarkable progression of outer retinal alterations, if comparing baseline (C) with 1-year follow-up (D), with increased window effect on structural OCT (*white arrow*), EZ disruption (*red square*), and fundus autofluorescence alterations (*orange square*).

Choroidal caverns identified in our RP cohort shared common features with those described in other diseases.[20] Interestingly, OCT-based choroidal patterns did not show any age effect. The three identified choroidal patterns revealed a correlation with clinical and OCT findings, with pattern 1 being characterized by the best phenotypical manifestation and pattern 3 by the worst one. The best phenotype in pattern 1 was also characterized by superior blood flow parameters, as indicated by higher VD and VT as well as lower VDisp and VR.[15]

The quantitative analysis of choroidal features revealed further details regarding the choroidal impairment in RP. In particular, the combined use of CSI and choroidal layers thickness provided evidence of an increased stromal area and a concomitant reduction of the choroidal vascular network. Interestingly, the pattern 1 cohort has the same vascular structure

Table 4. Progression Analysis in RP

Choroidal Pattern	1	2	3
Parameter	*P* Values (1 Year vs. Baseline)		
RNFL	>0.05	>0.05	>0.05
CMT	>0.05	>0.05	**0.03**
Choroidal thickness	>0.05	>0.05	>0.05
BCVA (logMAR)	>0.05	>0.05	**0.04**
VD mSCP	>0.05	>0.05	>0.05
VD mDCP	>0.05	>0.05	**0.02**
VD mCC	>0.05	>0.05	**<0.001**
VD RPC	>0.05	>0.05	>0.05
VD nSCP	>0.05	>0.05	**0.01**
VD nDCP	>0.05	>0.05	**0.03**
VD nCC	>0.05	>0.05	**0.03**
VDisp mSCP	>0.05	>0.05	>0.05
VDisp mDCP	>0.05	>0.05	>0.05
VDisp RPC	>0.05	>0.05	>0.05
VDisp nSCP	>0.05	>0.05	>0.05
VDisp nDCP	>0.05	>0.05	>0.05
VT mSCP	>0.05	>0.05	**<0.001**
VT mDCP	>0.05	>0.05	**0.01**
VT RPC	>0.05	>0.05	**<0.001**
VT nSCP	>0.05	>0.05	**0.03**
VT nDCP	>0.05	>0.05	>0.05
VR mSCP	>0.05	>0.05	**0.02**
VR mDCP	>0.05	>0.05	>0.05
VR RPC	>0.05	>0.05	**0.02**
VR nSCP	>0.05	>0.05	>0.05
VR nDCP	>0.05	>0.05	>0.05

Statistically significant changes are reported in bold numbers. "m" and "n" used for macular and optic nerve head vascular plexa, respectively.

as that of healthy participants, even with a significant choroidal thinning, mainly related to the reduction of Haller layers, whereas patients characterized by patterns 2 and 3 disclosed a globally altered choroidal structure. The subdivision into choroidal patterns disclosed a significant prognostic impact, as the pattern 3 cohort showed a significant worsening of BCVA as well as of vascular and nonvascular parameters. With respect to patterns 1 and 2, no significant changes have been found, and it is worth noticing that eyes with pattern 2, although worse with respect to pattern 1 patients at baseline, maintained their functional and anatomical conditions at 1-year follow-up.

Choroidal abnormalities could be explained by hypothesizing that the primary alterations at the level of the RPE/photoreceptor complex might lead to the loss of trophic stimuli to the vascular network, bringing about a progressive loss of both retinal and choroidal perfusions, followed by choroidal stromal changes.

We are aware that our study has several limitations. First, a quantitative OCTA analysis depends on high-quality images. Thus, patients showing OCTA-related artifacts cannot be analyzed.[21,22] On the other side, all the precautions were adopted to minimize the potential effect of these artifacts on data analysis. Another limitation is related to the fact that CSI measurement might be affected by possible increased reflectivity transmission on the choroid, secondary to RPE atrophy. In addition, we acknowledge that our quantitative imaging-based analysis would need a histopathologic validation. Moreover, the number of cases and the duration of the follow-up in our study are still too limited to draw any definitive conclusions, especially regarding the absence of an age effect. Last, no attempt was made to try a genotype-phenotype correlation due to the limited number of patients. Thus, our investigation should be considered a mere pilot study designed to stimulate larger prospective multicentric studies on the choroidal alterations in RP.

In conclusion, our study identified three choroidal patterns in RP, which are related to the retinal impairment and the visual acuity outcome. Choroidal patterns may provide useful information in terms of disease progression, thus showing a potential role in clinical settings. Further studies are warranted to better clarify the role of the choroid in RP.

Acknowledgments

Disclosure: **A. Arrigo**, None; **A. Bordato**, None; **F. Romano**, None; **E. Aragona**, None; **A. Grazioli**, None; **F. Bandello**, Allergan (C), Bayer Shering-Pharma (C), Hoffmann-La-Roche (C), NTC Pharma (C), Novartis (C), SIFI (C), SOOFT (C), Thrombogenics (C), Zeiss (C); **M. Battaglia Parodi**, None

References

1. Berson EL. Retinitis pigmentosa. The Friedenwald Lecture. *Invest Ophthalmol Vis Sci*. 1993;34:1659–1676.
2. Pagon RA. Retinitis pigmentosa. *Surv Ophthalmol*. 1968;33:137–177.
3. Van Soest S, Westerveld A, de Jong PT, Bleeker-Wagemakers EM, Bergen AA. Retinitis

pigmentosa: defined from a molecularpoint of view. *Surv Ophthalmol*. 1999;43:321–334.
4. Milam AH, Li ZY, Fariss RN. Histopathology of the human retina in retinitis pigmentosa. *Prog Retin Eye Res*. 1998;17:175–205.
5. Hartong DT, Berson EL, Dryja TP. Retinitis pigmentosa. *Lancet*. 2006;368:1795–1809.
6. Bunker CH, Berson EL, Bromley WC, Hayes RP, Roderick TH. Prevalence of retinitis pigmentosa in Maine. *Am J Ophthalmol*. 1984;97:357–365.
7. Grover S, Fishman GA, Anderson RJ, et al. Visual acuity impairment in patients with retinitis pigmentosa at age 45 years or older. *Ophthalmology*. 1999;106:1780–1785.
8. Berson EL, Sandberg MA, Rosner B, et al. Natural course of retinitis pigmentosa over a three-year interval. *Am J Ophthalmol*. 1985;99:240–251.
9. Milam AH, Li ZY, Fariss RN. Histopathology of the human retina in retinitis pigmentosa. *Prog Retin Eye Res*. 1998;17:175–205.
10. Battaglia Parodi M, Cicinelli MV, Rabiolo A, et al. Vessel density analysis in patients with retinitis pigmentosa by means of optical coherence tomography angiography. *Br J Ophthalmol*. 2017;101:428–432.
11. Guduru A, Al-Sheikh M, Gupta A, Ali H, Jalali S, Chhablani J. Quantitative assessment of the choriocapillaris in patients with retinitis pigmentosa and in healthy individuals using OCT angiography. *Ophthalmic Surg Lasers Imaging Retina*. 2018;49:e122–e128.
12. Mastropasqua R, Borrelli E, Agnifili L, et al. Radial peripapillary capillary network in patients with retinitis pigmentosa: an optical coherence tomography angiography study. *Front Neurol*. 2017;8:572.
13. Miyata M, Oishi A, Hasegawa T, et al. Concentric choriocapillaris flow deficits in retinitis pigmentosa detected using wide-angle swept-source optical coherence tomography angiography. *Invest Ophthalmol Vis Sci*. 2019;60:1044–1049.
14. Schindelin J, Arganda-Carreras I, Frise E, et al. Fiji: an open-source platform for biological-image analysis. *Nat Methods*. 2012;9:676–682.
15. Arrigo A, Aragona E, Capone L, et al. Advanced optical coherence tomography angiography analysis of age-related macular degeneration complicated by onset of unilateral choroidal neovascularization. *Am J Ophthalmol*. 2018;195:233–242.
16. Tan R, Agrawal R, Taduru S, Gupta A, Vupparaboina K, Chhablani J. Choroidal vascularity index in retinitis pigmentosa: an OCT study. *Ophthalmic Surg Lasers Imaging Retina*. 2018;49(3):191–197.
17. Battaglia Parodi M, La Spina C, Triolo G, et al. Correlation of SD-OCT findings and visual function in patients with retinitis pigmentosa. *Graefes Arch Clin Exp Ophthalmol*. 2016;254:1275–1279.
18. Dhoot DS, Huo S, Yuan A, et al. Evaluation of choroidal thickness in retinitis pigmentosa using enhanced depth imaging optical coherence tomography. *Br J Ophthalmol*. 2013;97:66–69.
19. Sodi A, Lenzetti C, Murro V, et al. EDI-OCT evaluation of choroidal thickness in retinitis pigmentosa. *Eur J Ophthalmol*. 2018;28:52–57.
20. Dolz-Marco R, Glover JP, Gal-Or O, et al. Choroidal and sub-retinal pigment epithelium caverns: multimodal imaging and correspondence with Friedman lipid globules. *Ophthalmology*. 2018;125:1287–1301.
21. Spaide RF, Fujimoto JG, Waheed NK. Image artifacts in optical coherence tomography angiography. *Retina*. 2015;35:2163–2180.
22. Spaide RF, Fujimoto JG, Waheed NK, Sadda SR, Staurenghi G. Optical coherence tomography angiography. *Prog Retin Eye Res*. 2018;64:1–55.